



City Research Online

## City, University of London Institutional Repository

---

**Citation:** Dong, H., Sui, M., Mu, G., Zhao, J., Li, T., Sun, T. & Grattan, K. T. V. (2023). Velocity and Direction Adjustment of Actuated Droplets Using the Standing Wave Ratio of Surface Acoustic Waves (SAW). *IEEE/ASME Transactions on Mechatronics*, 28(4), pp. 2399-2404. doi: 10.1109/tmech.2023.3237664

This is the accepted version of the paper.

This version of the publication may differ from the final published version.

---

**Permanent repository link:** <https://openaccess.city.ac.uk/id/eprint/30047/>

**Link to published version:** <https://doi.org/10.1109/tmech.2023.3237664>

**Copyright:** City Research Online aims to make research outputs of City, University of London available to a wider audience. Copyright and Moral Rights remain with the author(s) and/or copyright holders. URLs from City Research Online may be freely distributed and linked to.

**Reuse:** Copies of full items can be used for personal research or study, educational, or not-for-profit purposes without prior permission or charge. Provided that the authors, title and full bibliographic details are credited, a hyperlink and/or URL is given for the original metadata page and the content is not changed in any way.

---

City Research Online:

<http://openaccess.city.ac.uk/>

[publications@city.ac.uk](mailto:publications@city.ac.uk)

---

# Velocity and Direction Adjustment of Actuated Droplets Using the Standing Wave Ratio of Surface Acoustic Waves (SAW)

Huijuan Dong<sup>1</sup>, Mingyang Sui<sup>1</sup>, Guanyu Mu<sup>1</sup>, Jie Zhao<sup>1</sup>, *Member, IEEE*, Tianlong Li<sup>1</sup>, Tong Sun<sup>2</sup> and Kenneth T.V. Grattan<sup>1,2</sup>

**Abstract**—Droplet actuation using Surface Acoustic Wave (SAW) technology has recently been widely employed in ‘lab on a chip’ applications. In this paper, SAWs generated by Inter-Digital Transducers (IDTs) were used to actuate micro-droplets, where their velocity and direction could be adjusted by changing only the excitation phase shift,  $\theta$ , of the voltage applied to the two IDTs. Specifically, an analytical expression for the acoustic Standing Wave Ratio (SWR), operating in the Exciter-Exciter mode, has been derived by the authors, and given as a function of  $\theta$  and the spatial phase difference. It can be seen from the expression that the directions of the Traveling Surface Acoustic Waves (TSAWs) will be opposite to each other, in the range of  $\theta$  given by  $(0, \pi)$  and  $(\pi, 2\pi)$ , and the component of the TSAWs can be adjusted by changing  $\theta$  in each direction. Following the theoretical analysis discussed here, the IDTs fabricated on a LiNbO<sub>3</sub> substrate have been excited to generate a mixture of TSAWs and Standing Surface Acoustic Waves (SSAWs). A series of experiments was carried out to control the velocity and direction of the actuated droplets, by changing only  $\theta$ . In addition, an experiment performed to compare the techniques shows that the upper limit of the velocity of the actuated droplets can be significantly increased using the Exciter-Exciter mode, showing that it has the potential to be an alternative method to the routine Exciter-Absorber mode.

**Index Terms**—Surface Acoustic Wave (SAW), Inter-Digital Transducers (IDTs), Exciter-Exciter mode, excitation phase shift, Standing Wave Ratio (SWR)

## I. INTRODUCTION

Microfluidics has been widely used in chemical analysis and biomedical research<sup>[1-3]</sup>. By using this technique in the handling and manipulating of trace amounts of fluids, for example biological fluids on small chips which are a few square

centimeters in size, sample costs and processing times can be reduced and high-sensitivity separation and detection can be performed<sup>[4-5]</sup>. In such ‘lab-on-a-chip’ applications, droplet manipulation is an important branch of microfluidic technology. Over several decades, a variety of different approaches to actuate droplets on a substrate have been discussed and results published, including the use of techniques such as electrodynamics<sup>[6]</sup>, acoustics<sup>[7]</sup> and hydrodynamics<sup>[8]</sup>. Among these, droplet actuation using Surface Acoustic Wave (SAW) technology shows a number of important characteristics, such as convenience for modular integration, allowing the manipulation of droplets without direct contact, as well as scalability and programmability<sup>[9]</sup>. Drawing on these advantages, droplet actuation technology using a SAW-based method becomes a promising approach and thus has been widely employed in some ‘lab-on-a-chip’ applications<sup>[10]</sup>.

The Traveling Surface Acoustic Wave (TSAW)-based approach has also routinely been used to actuate droplets<sup>[4,11]</sup>. Specifically, TSAWs on the substrate can be generated when a single Inter-Digital Transducer (IDT) on a piezoelectric substrate is excited by an RF power source. Simultaneously, another IDT or an adhesive can be placed on the other edge of the substrate to absorb the vibration, where this can be called the Exciter-Absorber mode. When the droplet is placed in the propagation path of the TSAW, the acoustic energy can be radiated into the droplet to create a sufficiently large acoustic pressure gradient within it<sup>[12]</sup>. As a result, the droplet can be moved in the same direction as that in which the wave is propagating<sup>[13-15]</sup>.

In this work, the Exciter-Exciter mode (exciting a pair of opposing IDTs simultaneously) has been used for droplet actuation, in a way that is different from using the Exciter-Absorber mode. (In previous studies, the Exciter-Exciter mode could be used to generate a pure Standing Surface Acoustic Wave (SSAW) in a micro-channel which was placed on the substrate, where phase control of the opposing IDTs had previously been employed to change the positions of the

This work was supported in part by the National Natural Science Foundation of China under Grant 52275014 and in part by the support of the British Council through the “Going Global Partnerships—Enabling Grants to Strengthen U.K.-China Institutional Partnerships through academic collaboration 2021” programme. (*Corresponding author: Jie Zhao and K.T.V. Grattan*)

H. Dong, M. Sui, G. Mu, J. Zhao, T. Li and K.T.V. Grattan are with the State Key Laboratory of Robotics and System, Harbin Institute of Technology,

Harbin 150001, China (e-mail: dhj@hit.edu.cn; suimingyang97@outlook.com; muguanyu@hit.edu.cn; jzhao@hit.edu.cn; K.T.V.Grattan@city.ac.uk).

T. Sun and K.T.V. Grattan are with the School of Science & Technology, City, University of London, London, EC1V 0HB, UK (e-mail: t.sun@city.ac.uk; K.T.V.Grattan@city.ac.uk).

standing wave nodes and thus the particles captured by the nodes could be manipulated [16].) However, in the Exciter-Exciter mode reported here, considering the reflection of the surface acoustic wave from the IDTs in the SAW device without a micro-channel (which has usually been ignored in previous studies), the equation for the mechanical vibration of the mixed TSAWs and SSAWs formed on the substrate surface by using the Exciter-Exciter mode, are discussed for the first time. In the mixed waves, the TSAWs component can be adjusted by changing the excitation phase shift,  $\theta$ , of the voltage applied to the two opposite IDTs. Thus an adjustment of the velocity and direction of the actuated droplets can be achieved.

In this paper, an expression for the traveling wave component of the mixed waves has been derived by the authors (here the ratio of the *maximum* to the *minimum* vibration amplitude, defined as the Standing Wave Ratio (SWR), which was used to describe the traveling wave component [17]). As a result, a method for the control of the velocity and the direction of the actuated droplets, by using a knowledge of  $\theta$  to adjust the SWR, has been discussed. In addition, a series of experiments has then been carried out to modify the velocity and direction of the actuated droplets, where this approach has been shown to increase the velocity of the droplets.

## II. THEORETICAL BACKGROUND

It is well known that a pure standing wave, a pure traveling wave or a mixture of the two can be formed on a substrate [18-19], and the envelope diagrams of the vibrational waveforms are shown in Fig. 1. Different vibrational waveforms can be distinguished by the value of SWR (that is the ratio of the *maximum* to the *minimum* vibration amplitude). The value of SWR lies between unity and infinity when a mixed wave, comprising travelling waves and standing waves, is formed.

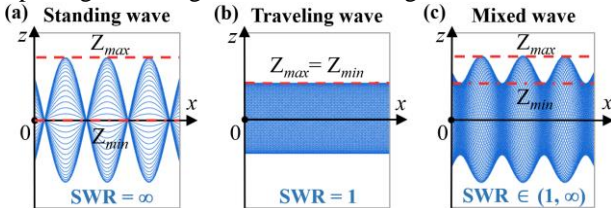


Fig. 1. Waveform envelope diagrams of the different types of vibration on the substrate. (a) the pure standing wave, (b) the pure traveling wave, (c) the mixed wave. The dashed lines show the maximum amplitudes ( $Z_{\max}$ ) of all the particles on the surface of the substrate, and the dash-dotted line shows the minimum amplitudes ( $Z_{\min}$ ), that is, the amplitude of the TSAW component.

In this study, the Exciter-Exciter mode has been used by the authors to excite a mixture of TSAWs and SSAWs, and the SWR is then used to describe the TSAW component in the mixed waves. It can be noted that the value of the SWR is related to the design parameters of the two IDTs and  $\theta$ . Several important specific theoretical relationships can be derived, as discussed below.

### A. Vibration of the mixed waves on the substrate surface

As shown in Fig. 2, the acoustic waves excited by each pair of fingers in an IDT are superimposed on each other, and this can be considered as the acoustic excitation source being positioned along the center line of each IDT. Here  $L$  represents

the distance between IDT 1 and IDT 2, as shown in Fig. 2. During the process of actuating the droplets, the two IDTs were excited at the same frequency and amplitude, with an excitation phase shift,  $\theta$ . It is assumed that the incident wave excited by the IDT on one side will be totally reflected back after propagating to the IDT on the other side.

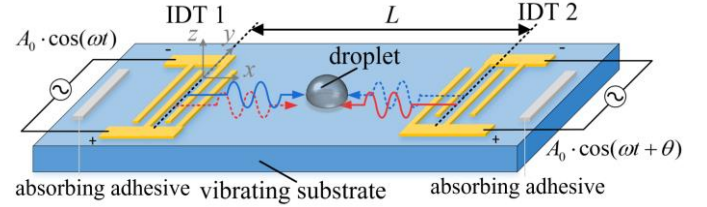


Fig. 2. Schematic of the Exciter-Exciter mode of the droplet actuation device using the SAW. Here the blue solid line and the blue dotted line represent the incident wave,  $A_0 \cos(\omega t)$ , excited by IDT 1 and its reflected wave respectively (where  $A_0$  represents the amplitude of the TSAW generated by one IDT). Similarly, the red solid line and the red dotted line represent the incident wave excited by IDT 2,  $A_0 \cos(\omega t + \theta)$ , and its reflected wave respectively.

As illustrated in Fig. 2, IDT 1 generates a traveling incident wave which will be totally reflected from the other side of the device, forming a traveling reflected wave. Similarly, IDT 2 generates a traveling incident wave and a reflected wave. Following that, these four traveling waves are superimposed to form two standing waves, which are then superimposed on each other. Thus the  $z$  direction-based vibrational displacement of each particle on the surface of the substrate at time,  $t$ , and at a position,  $x$ , can be written as [18,20-22]:

$$Z(x, t) = 2A_0 [\cos \omega t \cos kx + \cos(\omega t + \theta) \cos(kx + kL)] \quad (1)$$

where  $\omega$  and  $k$  respectively represent the angular frequency applied to both the IDTs and the wavenumber of the vibrational displacement and  $\theta$  is the excitation phase shift of the voltage. To more easily derive the following equations,  $\alpha$  is termed as the spatial phase difference, given by  $k(L - n\frac{c}{f})$ , where  $c$  and  $f$  respectively represent the speed of sound in the SAW, propagating on the substrate and the frequency of the excitation signals, and  $n$  is an integer where  $\alpha \in [0, 2\pi)$ ; thus, the term  $\cos(kx + kL)$  is numerically equivalent to  $\cos(kx + \alpha)$ .

### B. Standing Wave Ratio (SWR)

To obtain the value of the SWR, it is necessary to calculate both the maximum and minimum vibrational amplitudes from Equation (1), respectively being  $Z_{x \max}$  and  $Z_{x \min}$ , of  $Z(x, t)$ , which can be derived from Equation (1) and these are given by:

$$Z_{x \max} = \begin{cases} 2A_0 \left| 2 \cos \frac{\alpha}{2} \cos \frac{\theta}{2} \right| & (0 < \theta < \theta_1, \quad \theta_2 < \theta < 2\pi) \\ 2A_0 \left| 2 \sin \frac{\alpha}{2} \sin \frac{\theta}{2} \right| & (\theta_1 \leq \theta \leq \theta_2) \end{cases} \quad (2)$$

$$Z_{x \min} = \begin{cases} 2A_0 \left| 2 \sin \frac{\alpha}{2} \sin \frac{\theta}{2} \right| & (0 < \theta < \theta_1, \quad \theta_2 < \theta < 2\pi) \\ 2A_0 \left| 2 \cos \frac{\alpha}{2} \cos \frac{\theta}{2} \right| & (\theta_1 \leq \theta \leq \theta_2) \end{cases}$$

where  $\theta_1$  and  $\theta_2$  are the two values of  $\theta$  seen when  $Z_{x \max} = Z_{x \min}$ , that is, when the pure TSAW is produced, which can be expressed as shown below:

$$\theta_1 = \begin{cases} \pi - \alpha & (0 \leq \alpha \leq \pi) \\ \alpha - \pi & (\pi < \alpha \leq 2\pi) \end{cases}$$

$$\theta_2 = \begin{cases} \pi + \alpha & (0 \leq \alpha \leq \pi) \\ 3\pi - \alpha & (\pi < \alpha \leq 2\pi) \end{cases}$$

This allows the  $1/\text{SWR}$  of the SAW forming on the substrate to be expressed as shown below, which can be seen to be related to both  $\theta$  and  $\alpha$ .

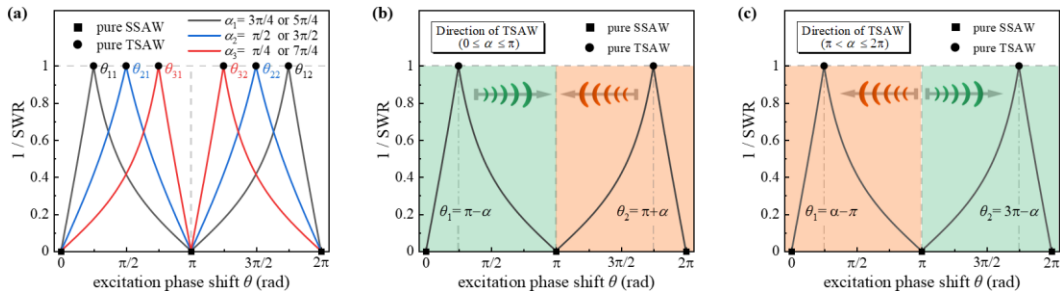
$$\frac{1}{\text{SWR}} = \frac{Z_{x\min}}{Z_{x\max}} = \begin{cases} 0 & (\theta = 0, \pi, 2\pi) \\ \left| \tan \frac{\alpha}{2} \tan \frac{\theta}{2} \right| & (0 < \theta < \theta_1, \theta_2 < \theta < 2\pi) \\ 1 & (\theta = \theta_1, \theta_2) \\ \left| \cot \frac{\alpha}{2} \cot \frac{\theta}{2} \right| & (\theta_1 < \theta < \theta_2) \end{cases} \quad (3)$$

As can be seen from Equation (3), the larger is  $1/\text{SWR}$ , the more is the traveling wave component. It can be noted that when the IDTs are prepared, the distance between the two IDTs,  $L$ , and the sound speed of the SAW,  $c$ , are constant. Then the value of  $\alpha$  will also remain unchanged if the frequency of the excitation signals,  $f$ , remains constant. In this case, the value of the SWR can be controlled by adjusting  $\theta$  only.

### C. Velocity adjustment of the actuated droplets by changing the SWR

Based on the analytical expressions for the SWR,  $\theta$  and  $\alpha$  given above, the curves illustrating the relationship across  $\theta$  and the SWR, for different values of  $\alpha$ , are shown in Fig. 3(a). It can be clearly seen that not only can the pure TSAWs be created for two values of  $\theta$ , but also the pure SSAWs can be similarly formed, where  $\theta$  is given by 0 or  $\pi$ . It can be noted that the two values of  $\theta$  being used to produce the pure TSAWs are related to  $\alpha$ , while those being used to create the pure SSAWs have constant values of  $\theta$ , these being 0 and  $\pi$ , and independent of  $\alpha$ . In addition, for a given value of  $\alpha$ , in either of the ranges,  $(0 < \theta < \pi)$  or  $(\pi < \theta < 2\pi)$ , the traveling wave component (that is the  $1/\text{SWR}$ ) of the SAW can be adjusted by changing  $\theta$  only.

It can be noted that in the mixed waves, formed from TSAWs and SSAWs, only the TSAWs can drive the droplets, while the SSAWs cannot [11]. Furthermore, previous studies have shown that the larger the amplitudes of the TSAWs, the faster will be the velocity of the actuated droplets [23-25]. Therefore, the larger the value of  $1/\text{SWR}$ , the closer  $\theta$  (in Fig. 3(a)) will be to  $\theta_1$  or  $\theta_2$ , and the faster the actuated droplets will move. As can be seen, the droplets reach their greatest velocity when  $\theta$  equals  $\theta_1$  or  $\theta_2$ , while the droplets will be stationary when  $\theta$  equals 0,  $\pi$  or  $2\pi$ . In this way, the velocity of the actuated droplets can be adjusted by changing  $\theta$ .



In addition as can be seen from Equation (2), for a given value of  $\alpha$ , pure TSAWs can be formed when  $\theta$  is set to  $\theta_1$  or  $\theta_2$ , where the relative maximum value of the amplitude of the TSAWs ( $Z_{x\min}$ ),  $Z_{\text{pure TSAW}}$ , can be obtained as:

$$Z_{\text{pure TSAW}} = 2A_0 |\sin \alpha| \quad (4)$$

As illustrated by Equation (4), the amplitudes of the pure TSAWs,  $Z_{\text{pure TSAW}}$ , vary with the values of  $\alpha$ , and  $Z_{\text{pure TSAW}}$  is greater than  $A_0$  (the amplitude of the TSAW excited by one single IDT) when  $\alpha$  is set to be in the ranges of  $(\pi/6, 5\pi/6)$  or  $(7\pi/6, 11\pi/6)$ . In other words, assuming that the amplitude of the TSAW is  $A_0$  when exciting one IDT with a certain voltage ( $V_{\text{pp}}$ ) in the Exciter-Absorber mode, then the amplitude of the TSAW generated could exceed  $A_0$  or even reach  $2A_0$  when exciting a pair of IDTs with  $V_{\text{pp}}$  in the Exciter-Exciter mode, using an appropriate value of  $\alpha$ . In summary therefore, a larger TSAW amplitude can be generated by using the Exciter-Exciter mode compared with the Exciter-Absorber mode with the same input voltage. Previous studies have shown that the droplet will move faster under driving with the TSAW with larger amplitude [23-25]. Thus, the upper limit of the droplet velocity can be significantly increased due to the increase of the amplitude of the TSAW by using the Exciter-Exciter mode.

### D. Direction change of the actuated droplets using the SWR

Here the directions of the pure TSAWs can be further derived. Taking  $\alpha_1 = 3\pi/4$  or  $5\pi/4$  as an example (the curve shown in gray in Fig. 3(a)), when  $\theta$  is given by  $\theta_{11}$  or  $\theta_{12}$ , the pure TSAWs can be formed on the substrate and the normalized vibrational displacement can be written as:

$$\hat{Z}(x,t) = \begin{cases} \sin \alpha_1 \sin(kx - \omega t + \alpha_1) & (\theta = \theta_{11}, \alpha_1 = 3\pi/4 \in [0, \pi]) \\ \sin \alpha_1 \sin(kx + \omega t + \alpha_1) & (\theta = \theta_{12}, \alpha_1 = 3\pi/4 \in [0, \pi]) \\ \sin \alpha_1 \sin(kx + \omega t + \alpha_1) & (\theta = \theta_{11}, \alpha_1 = 5\pi/4 \in (\pi, 2\pi]) \\ \sin \alpha_1 \sin(kx - \omega t + \alpha_1) & (\theta = \theta_{12}, \alpha_1 = 5\pi/4 \in (\pi, 2\pi]) \end{cases} \quad (5)$$

It can be seen from Equation (5) that the directions of the pure TSAWs at  $\theta_1$  and  $\theta_2$  are opposite to each other. Furthermore, the direction of the TSAW in the range where  $\theta$  varies from 0 to  $\pi$  is identical to that at  $\theta_1$ , while the TSAW direction in the range of  $\theta$  varying from  $\pi$  to  $2\pi$  is identical to that at  $\theta_2$ . Therefore, considering the two cases of  $0 \leq \alpha \leq \pi$  and  $\pi < \alpha \leq 2\pi$ , the relationships between  $\theta$  and the directions of the corresponding TSAW components are shown in Fig. 3(b) and (c). It can be concluded that the direction change of the TSAW components can be realized by adjusting  $\theta$  as shown  $(0 < \theta < \pi)$  or  $(\pi < \theta < 2\pi)$ .

Fig. 3. (a) Theoretical relationships between  $\theta$  and  $1/\text{SWR}$  under different  $\alpha$  conditions. Here the squares and the solid circles used represent the pure SSAW and the pure TSAW respectively.  $\theta_{11}$  and  $\theta_{12}$  are the excitation phase shifts that were used to excite the pure TSAWs where  $\alpha_1=3\pi/4$  or  $5\pi/4$ . Similarly,  $\theta_{21}$  and  $\theta_{22}$ ,  $\theta_{31}$  and  $\theta_{32}$  correspond to  $\alpha_2=\pi/2$  or  $3\pi/2$ ,  $\alpha_3=\pi/4$  or  $7\pi/4$  respectively. (b) and (c) Relationships between  $\theta$  and the directions of the traveling waves components, where  $\alpha=3\pi/4$  in (b) and  $\alpha=5\pi/4$  in (c). Here the green and the orange areas represent the positive and negative x-directions respectively.

In summary, using the expressions derived for the SWR of the SAW on the vibrating substrate, a clear relationship across  $\theta$ ,  $\alpha$ , and  $1/\text{SWR}$  can be obtained. After determining the value of  $\alpha$  according to the geometrical parameters of the IDTs, the TSAW component (that is,  $1/\text{SWR}$ ) can be precisely controlled by changing  $\theta$ . Thus the velocity and the direction of actuated droplets can be adjusted in this way.

### III. DEVICE FABRICATION AND SYSTEM SETUP

The experimental system used in this study is shown in Fig. 4. Specifically, a SAW generator developed by the authors was used to create two excitation signals with an adjustable phase shift, and these were applied to the IDTs of the SAW-based micro-manipulation device placed on the IDT-driver board. Further, the mixed TSAWs and SSAWs can be excited on the vibrating  $\text{LiNbO}_3$  substrate of the SAW device, and thus the droplet on the substrate can be driven by the SAW. Here the IDT-driver board used was a specially designed PCB board which included two input signal ports, the driver circuitry for the SAW device, the test points and the SAW device placement area. The SAW device could be connected not only to the SAW generator to excite the IDTs, but also to the oscilloscope to measure their voltages. The steps taken in the manufacture of this SAW micro-manipulation devices were as follows: a double layer of chromium and gold (Cr, 5nm / Au, 80nm) was deposited on a photoresist-patterned  $128^\circ$  YX  $\text{LiNbO}_3$  wafer, followed by using lift-off technology to form a pair of IDTs. The IDTs were excited at a frequency of 39.5MHz in the experiments carried out.



Fig. 4. Photographs of the SAW generator and the IDT-driver board. Here the SAW-based micro-manipulation device was placed on the IDT-driver board, and an enlarged photograph of this is shown in the right side of this figure. A schematic of the structure of each IDT is shown in the blue dotted box. Here each IDT was made up of 30 pairs of electrodes which were fabricated in parallel and spaced uniformly on the substrate, where the acoustic aperture,  $P=6\text{mm}$  and the interdigital period,  $M=100\mu\text{m}$ .

### IV. EXPERIMENTAL STUDY

#### A. Relative change of the $1/\text{SWR}$ value of the surface acoustic waves

In order to assess the relative change of the actual  $1/\text{SWR}$  of the vibrating surface of the substrate, a method using the energy flow perspective has been proposed in this paper. Specifically, the SAW propagating on the substrate can generate a potential on the IDT through the piezoelectric effect, so the terminal

voltage of each IDT was equal to the sum of the potential and the excitation signal voltages. From such an energy flow perspective, the propagation of the traveling waves could be regarded as equivalent to the flow of mechanical energy. Therefore, the relative change of the actual value of the  $1/\text{SWR}$  of the vibrating surface could be assessed by comparing the amplitudes of the voltages of the two IDTs, which represent their potential energies.

In the experiment carried out, two sinusoidal RF signals with identical amplitudes of 18V and the same frequencies of 39.50MHz were respectively applied to the two IDTs, when the excitation phase shift,  $\theta$ , varied from  $0^\circ$  to  $360^\circ$ . After that, the voltages on the two IDTs were obtained by using the oscilloscope connected to them. In this way, the data representing the changing voltage amplitudes of the two IDTs, varying with  $\theta$ , were acquired and the results were plotted in Fig. 5(a). It can be seen that as  $\theta$  varies from  $0^\circ$  to  $360^\circ$ , the values of the voltage amplitudes of IDT 1 and IDT 2 both vary from 8V to 25V, showing different trends which are similar in form to sinusoidal curves, where the values of the voltage amplitudes of the two IDTs were not equal to each other.

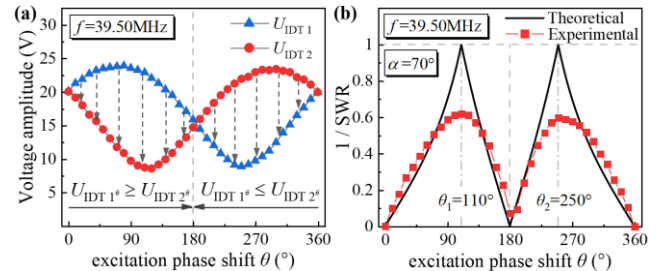


Fig. 5. (a) Measured voltage amplitudes of IDT 1 and IDT 2 plotted against  $\theta$ .  $\theta$  varied from  $0^\circ$  to  $360^\circ$ , in intervals of  $10^\circ$ , where the blue triangles and red circles represent the measured values of the voltage amplitudes of IDT 1 and IDT 2 respectively. (b) Experimental and theoretical values of  $1/\text{SWR}$  plotted against  $\theta$ , where  $f=39.50\text{MHz}$  and  $\alpha=70^\circ$ . The red squares represent the experimental relative values of the  $1/\text{SWR}$ , and the corresponding black lines denote the theoretical relationships.

In this work, the maximum and minimum values of the voltage amplitudes across IDT 1 and IDT 2 for a given value of  $\theta$  were recorded as  $U_{\text{max}}$  and  $U_{\text{min}}$  respectively. Here the traveling waves and the standing waves could be represented by  $U_{\text{max}} - U_{\text{min}}$  and  $U_{\text{min}}$  respectively, and the mixed waves by  $U_{\text{max}}$ . As a result, the actual measured value of  $1/\text{SWR}$  can be expressed as  $(U_{\text{max}} - U_{\text{min}})/U_{\text{max}}$ . In this way, the data showing the experimental and the theoretical values of  $1/\text{SWR}$  for different values of  $f$ , varying with  $\theta$  were acquired, as plotted in Fig. 5(b). As can be seen, the relative experimental values of  $1/\text{SWR}$  (which means the traveling wave components), have reached their relative maxima at  $\theta_1=110^\circ$  and  $\theta_2=250^\circ$ . Additionally, pure TSAWs could not be formed due to the incompletely reflected waves. Therefore, the SSAWs will always remain on the substrate and this will result in the maximum experimental values of the  $1/\text{SWR}$  seen being less than 1.

It can be seen from Fig. 5(a) and (b) that, in the range

$0^\circ < \theta < 180^\circ$ , the values of the voltage amplitudes of IDT 1 were larger than those of IDT 2, which meant that the traveling waves propagated from IDT 1 to IDT 2, and vice versa, for  $180^\circ < \theta < 360^\circ$ . This shows that the TSAWs components over these two ranges of  $\theta$  ( $0^\circ < \theta < 180^\circ$  and  $180^\circ < \theta < 360^\circ$ ), have opposite directions.

### B. Velocity adjustment and direction change of actuated droplets by changing $\theta$

Here the SAW-based micro-manipulation device has been used to actuate the droplets, and the velocity adjustment and directional change of the actuated droplets have been realized by changing the excitation phase shift,  $\theta$ . In these experiments, ethanol droplets were loaded on the substrate and driven by the SAW (water droplets could also be driven in the same way, but ethanol droplets were easier to actuate and a wider adjustment range for  $\theta$  is possible when changing the velocities of these ethanol droplets). Here the droplets were loaded on the LiNbO<sub>3</sub> substrate using a micropipette, keeping each droplet to have a volume of  $\sim 1\mu\text{L}$ , with its diameter ranging from 1000 to 1500 $\mu\text{m}$ . The movements of the droplets were captured and recorded by a high-speed camera (type GS3-U3-51S5C-C, FLIR), operating at 60 frames per second.

Here two sinusoidal RF signals with the same amplitudes ( $V_{pp}$ ) of 18V, the same frequency of 39.50MHz, as well as an excitation phase shift,  $\theta$ , varying from  $0^\circ$  to  $360^\circ$ , were respectively applied to the two IDTs to actuate the droplets. Following that, the absolute values of the velocities of the droplets were extracted from the videos recorded and plotted in Fig. 6, with a variety of different values of  $\theta$  being used. Photographs illustrating the movements of the actuated droplets are shown in both sides of Fig. 6. It can be seen that the droplet moved along the positive  $x$ -direction in the case of  $0^\circ < \theta < 180^\circ$ , and vice versa, for  $180^\circ < \theta < 360^\circ$ . In this way, it can be noted that a change in the direction of the droplets is possible by adjusting the value of  $\theta$ .

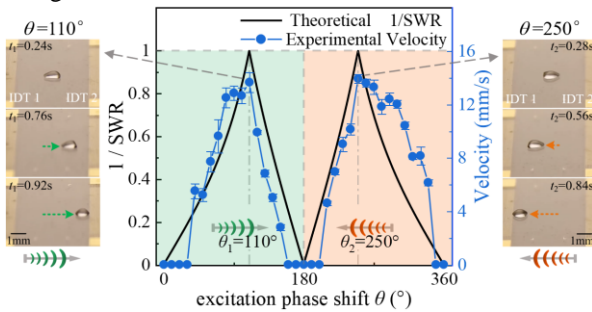


Fig. 6. Absolute values of the velocities of the droplets and the theoretical curve for the  $1/\text{SWR}$ .  $\theta$  varies from  $0^\circ$  to  $360^\circ$ , in intervals of  $10^\circ$ , where  $f=39.50\text{MHz}$ , and  $V_{pp}=18\text{V}$ . The blue points represent the absolute values of the velocities, and the black lines denote the theoretical values of  $1/\text{SWR}$ . Each average value of the velocity was obtained over four measurements being taken. Photographs of the movements of the actuation of the droplets in the positive  $x$ -direction when  $\theta=110^\circ$ , are shown on the left-hand side of this figure (with the time increasing from the top to the bottom of the set of photographs), while the droplets were driven in the negative  $x$ -direction when  $\theta=250^\circ$ , as shown on the right-hand side of the figure.

As can be seen from Fig. 6, these values of the droplet velocities fit well with the theoretical curve. The TSAW components are too small to overcome the friction present when  $\theta$  was programmed in the ranges of  $[0^\circ, 30^\circ]$  or  $[160^\circ, 200^\circ]$  or

$[350^\circ, 360^\circ]$  and as a result, the droplets could not be actuated. In addition, the actuated droplets reached their maximum velocities (which were 12.9mm/s and 13.9mm/s in their own directions), when  $\theta$  was equal to  $110^\circ$  and  $250^\circ$ , respectively. Here the two values of  $\theta$  which could theoretically form pure TSAWs, where the largest values of the traveling wave components were seen, are symmetric about  $\pi$ . Thus, it is possible to change the velocities of the droplets in the range from 2.8mm/s to 13.9mm/s by changing  $\theta$  only.

The experiments carried out have demonstrated that the velocity and the direction of the droplet can be adjusted by changing the value of one parameter,  $\theta$ , only, using the Exciter-Exciter mode. However, when using the Exciter-Absorber mode, it was necessary to control the on-off and amplitude of the excitation signals of two IDTs respectively, in order to achieve the same purpose which was an adjustment of the velocity and direction of the droplets. Therefore, the Exciter-Exciter mode used here can improve the convenience of the manual adjustment and the programmability.

### C. Comparison of the velocity of droplets actuated in the Exciter-Exciter mode and the Exciter-Absorber mode

As discussed in Section II, a larger amplitude of the pure TSAW can be formed (with the same input voltage) using the Exciter-Exciter mode proposed in this study, compared to the use of the Exciter-Absorber mode, as this can make the actuated droplet move more quickly. As was seen from the experimental results,  $\alpha$  is equal to  $70^\circ$  when  $f$  is given by 39.50MHz, using the SAW device here excited in the Exciter-Exciter mode. Thus, it can be calculated that  $Z_{\text{pure TSAW}}$  is equal to  $1.88A_0$ , which means, the maximum amplitude of the TSAW that can be excited under this condition is theoretically 1.88 times of the TSAW amplitude excited by the Exciter-Absorber mode.

The relationships between the velocities and  $V_{pp}$  under these two modes were measured on the SAW device developed here, and results are shown in Fig. 7. Here each point represents the average value of the velocities of the droplet moving in the positive and negative  $x$ -directions. As can be seen in Fig. 7, the average velocities of the droplets actuated in the Exciter-Exciter mode reached 34.27mm/s (at  $V_{pp}$  equal to 24V), compared to values of only 19.94mm/s in the Exciter-Absorber mode. It can be concluded that the upper limits of the velocities of the droplets could be raised by 72% for this SAW device using the Exciter-Exciter mode.

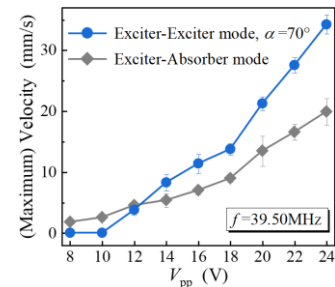


Fig. 7. Relationships between the average maximum velocities in the positive / negative directions and the input voltage,  $V_{pp}$ , in the Exciter-Absorber mode and Exciter-Exciter mode.  $V_{pp}$  varies from 8V to 24V, in intervals of 2V, where  $f=39.50\text{MHz}$ . The points shown as diamonds represent the average values of the velocities of the droplets actuated in the Exciter-Absorber mode, and the

points shown as dots represent the average maximum values of the velocities of the droplets, actuated in the Exciter-Exciter mode. When using the Exciter-Exciter mode, with the increase of the value of  $V_{pp}$ , the proportion of the remaining SSAWs decreases, and the vibration formed on the substrate was closer to that of the pure TSAW. As a result, the maximum velocities of the actuated droplets can be seen gradually to become greater than those in the Exciter-Absorber mode.

As a result, an improvement in the velocity of the actuated droplet, when using the Exciter-Exciter mode has been seen. Thus when the actuated droplet cannot reach the velocity required by using the Exciter-Absorber mode (corresponding to the maximum output voltage of the SAW generator), this Exciter-Exciter mode can be used significantly to improve the upper limit of the velocity achieved by the actuated droplet.

## V. CONCLUSION

In this paper, it has been reported for the first time that a mixture of Standing Surface Acoustic Waves (SSAWs) and Traveling Surface Acoustic Waves (TSAWs) can be excited on the substrate by using the Exciter-Exciter mode to actuate the droplets. Specifically, the analytical expression for the acoustic Standing Wave Ratio (SWR), operating in the Exciter-Exciter mode, has been derived by the authors and given as a function of the excitation phase shift,  $\theta$ , and the spatial phase difference. Following the theoretical analysis discussed, the excitation signals with the same amplitudes, frequencies but different phase shifts were applied to the two IDTs fabricated on a LiNbO<sub>3</sub> substrate, to generate a mixture of TSAWs and SSAWs. Then a series of experiments was carried out to achieve the adjustment of the velocity and direction of the actuated droplets, by changing  $\theta$  only. As a result, the actuated droplets reached their maximum velocity under the condition where, theoretically, pure TSAWs can be formed. The closer were the values of  $\theta$  set to 0° or 180°, the slower would be the movements of the droplets. Here the droplets moved in the opposite directions when  $\theta$  was set to be in the ranges of (0°, 180°) and (180°, 360°). In addition, the experimental results of the comparative study carried out indicate that the upper limit of the velocity of the droplet actuated in the Exciter-Exciter mode was 72% higher than that in the Exciter-Absorber mode, when the input voltage reached 24V.

These experimental results have demonstrated two advantages of the use of the Exciter-Exciter mode to actuate droplets, compared with the routinely used Exciter-Absorber mode, based on the SAW technology. These results emphasize that (1) the adjustment of the velocity and direction of the actuated droplets can be achieved by changing only one excitation parameter, allowing the greater convenience and programmability that is seen and (2) the velocity of the actuated droplets could be increased. Thus, this Exciter-Exciter mode approach has the potential to be a very useful alternative method to the routine Exciter-Absorber mode, and may further be applied to actuate micro-droplets in a range of biological and chemical applications, such as the on-chip PCR and for the merging of the sample droplets.

## REFERENCES

- [1] A. Demircali, R. Varol, G. Aydemir, E. N. Saruhan, K. Erkan, and H. Uvet, "Longitudinal Motion Modeling and Experimental Verification of a Microrobot Subject to Liquid Laminar Flow," *IEEE/ASME Transactions on Mechatronics*, pp. 1-1, 2021.
- [2] P. Li and T. J. Huang, "Applications of Acoustofluidics in Bioanalytical Chemistry," *Anal Chem*, vol. 91, no. 1, pp. 757-767, Jan. 2018.
- [3] J. Li *et al.*, "Magneto-Acoustic Hybrid Nanomotor," *Nano Lett*, vol. 15, no. 7, pp. 4814-21, Jul. 2015.
- [4] A. Wixforth, C. Strobl, C. Gauer, A. Toegl, J. Scriba, and Z. v Guttenberg, "Acoustic manipulation of small droplets," *Anal Bioanal Chem*, vol. 379, no. 7-8, pp. 982-91, Aug. 2004.
- [5] T. Xu *et al.*, "Reversible swarming and separation of self-propelled chemically powered nanomotors under acoustic fields," *J Am Chem Soc*, vol. 137, no. 6, pp. 2163-6, Feb. 2015.
- [6] C. L. Song *et al.*, "Fluid pumping by liquid metal droplet utilizing ac electric field," *Phys Rev E*, vol. 105, no. 2-2, p. 025102, Feb 2022.
- [7] R. Tao *et al.*, "Hierarchical Nanotexturing Enables Acoustofluidics on Slippery yet Sticky, Flexible Surfaces," *Nano Lett*, vol. 20, no. 5, pp. 3263-3270, May 13 2020.
- [8] S. Y. Teh, R. Lin, L. H. Hung, and A. P. Lee, "Droplet microfluidics," *Lab Chip*, vol. 8, no. 2, pp. 198-220, Feb. 2008.
- [9] S. P. Zhang *et al.*, "Digital acoustofluidics enables contactless and programmable liquid handling," *Nat Commun*, vol. 9, no. 1, p. 2928, Jul. 2018.
- [10] X. Ding *et al.*, "Surface acoustic wave microfluidics," *Lab Chip*, vol. 13, no. 18, pp. 3626-49, Sep. 2013.
- [11] Y. Ai and B. L. Marrone, "Droplet translocation by focused surface acoustic waves," *Microfluidics and Nanofluidics*, vol. 13, no. 5, pp. 715-722, 2012.
- [12] Z. J. Jiao, X. Y. Huang, and N. T. Nguyen, "Scattering and attenuation of surface acoustic waves in droplet actuation," *Journal of Physics A: Mathematical and Theoretical*, vol. 41, no. 35, 2008.
- [13] M. K. Tan, J. R. Friend, and L. Y. Yeo, "Interfacial jetting phenomena induced by focused surface vibrations," *Phys Rev Lett*, vol. 103, no. 2, p. 024501, Jul 2009.
- [14] S. B. Burnside, K. Pasieczynski, A. Zarareh, M. Mehmood, Y. Q. Fu, and B. Chen, "Simulations of surface acoustic wave interactions on a sessile droplet using a three-dimensional multiphase lattice Boltzmann model," *Phys Rev E*, vol. 104, no. 4-2, p. 045301, Oct 2021.
- [15] P. Brunet and M. Baudoin, "Unstationary dynamics of drops subjected to MHz-surface acoustic waves modulated at low frequency," *Experiments in Fluids*, vol. 63, no. 1, 2022.
- [16] G. Simon *et al.*, "Particle separation by phase modulated surface acoustic waves," *Biomicrofluidics*, vol. 11, no. 5, p. 054115, Sep 2017.
- [17] K. F. Graff, *Wave motion in elastic solids*. New York, USA: Dover, 1991, pp. 180-191.
- [18] T. Ide, J. R. Friend, K. Nakamura, and S. Ueha, "A Low-Profile Design for the Noncontact Ultrasonically Levitated Stage," *Japanese Journal of Applied Physics*, vol. 44, no. 6B, pp. 4662-4665, 2005.
- [19] D. Koyama, T. Ide, J. R. Friend, K. Nakamura, and S. Ueha, "An ultrasonically levitated noncontact stage using traveling vibrations on precision ceramic guide rails," *IEEE Trans Ultrason Ferroelectr Freq Control*, vol. 54, no. 3, pp. 597-604, Mar 2007.
- [20] J. Zhao, G. Mu, H. Dong, T. Sun, and K. T. V. Grattan, "Requirements for a transportation system based on ultrasonic traveling waves using the measurement of spatial phase difference," *Mechanical Systems and Signal Processing*, vol. 168, 2022.
- [21] C. Chen, J. S. Wang, B. Jia, and F. Li, "Design of a noncontact spherical bearing based on near-field acoustic levitation," *Journal of Intelligent Material Systems and Structures*, vol. 25, no. 6, pp. 755-767, Apr 2014.
- [22] J. Zhao, G. Mu, H. Dong, T. Sun, and K. T. V. Grattan, "Study of the Velocity and Direction of Piezoelectric Robot Driven by Traveling Waves," *IEEE Transactions on Industrial Electronics*, 2022.
- [23] M. S. Noori, M. T. Rahni, and A. S. Taleghani, "Effects of contact angle hysteresis on drop manipulation using surface acoustic waves," *Theoretical and Computational Fluid Dynamics*, vol. 34, no. 1-2, pp. 145-162, 2020.
- [24] P. Brunet, M. Baudoin, O. B. Matar, and F. Zoueshtyagh, "Droplet displacements and oscillations induced by ultrasonic surface acoustic waves: a quantitative study," *Phys Rev E Stat Nonlin Soft Matter Phys*, vol. 81, no. 3 Pt 2, p. 036315, Mar 2010.

- [25] M. Baudoin, P. Brunet, O. Bou Matar, and E. Herth, "Low power sessile droplets actuation via modulated surface acoustic waves," *Applied Physics Letters*, vol. 100, no. 15, 2012.